MID-INFRARED SPECTRA OF SYTHETIC PYROXENES OVER THE ENTIRE Ca-Mg-Fe QUADRILATERAL. M. D. Lane[1], R. L. Klima[2], T. D. Glotch[3], and M. D. Dyar[4,5], [1]Fibernetics LLC (Lititz, PA, lane@fibergyro.com), [2]Johns Hopkins University Applied Physics Laboratory (Laurel, MD), [3]Stony Brook University (Stony Brook, NY), [4]Planetary Science Institute, (Tucson, AZ), [5]Mount Holyoke College (South Hadley, MA).

Introduction: Pyroxene minerals are some of the most abundant minerals in the solar system and are plentiful in meteorites and other igneous rocks. They form under distinct chemical and environmental conditions enabling them to be used as geothermometers for interpreting magmatic evolution and cooling history [e.g., 1-4].

Pyroxene compositions are generally written as $XY(Si,Al)_2O_6$. where X represents the cations in a generally distorted octahedral coordination (M2 site), Y represents the smaller cations in the regular octahedral M1 site, and Si and Al are found in the tetrahedral site. In their simplest form pyroxenes contain single SiO_3 chains of linked SiO_4 tetrahedra.

Mid-infrared (5-50 microns; 2000-200 cm^{-1}) spectroscopic studies of natural pyroxenes are fairly common using absorption, reflectance, or emission spectroscopy [e.g., 5-9] and have been used to link mineral structure to spectral character. These natural samples contained additional cations (e.g., Na^+, Zn^{2+}, Cr^{3+}, etc.). For this study, however, we use synthetic pyroxene samples, limiting the chemistries studied to the Ca^{2+}, Mg^{2+}, and Fe^{2+} "pyroxene quadrilateral"– the lower half of the wollastonite-enstatite-ferrosilite ternary where Ca^{2+} is limited to 50 mol% or less because Ca is large and unable to occupy the M1 site (Fig. 1). Enstatite is the Mg endmember; ferrosilite is the Fe endmember. Along this Mg-Fe join are the (orthorhombic) orthopyroxenes. Above this join are the (monoclinic) clinopyroxenes.

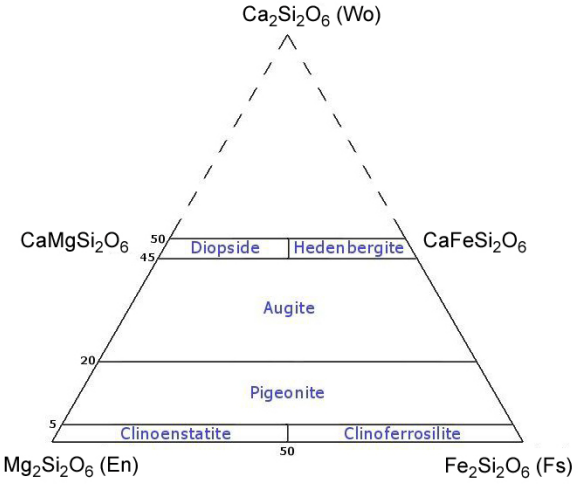

Figure 1. Compositional ranges of Ca-Mg-Fe pyroxenes and their accepted nomenclature.

Samples for Spectral Study: The 62 samples measured for this study were synthesized by Dr. Don Lindsley and colleagues (Stony Brook U.) and represent diverse pyroxene chemical compositions (Table 1) over the entire pyroxene quadrilateral (Fig. 2).

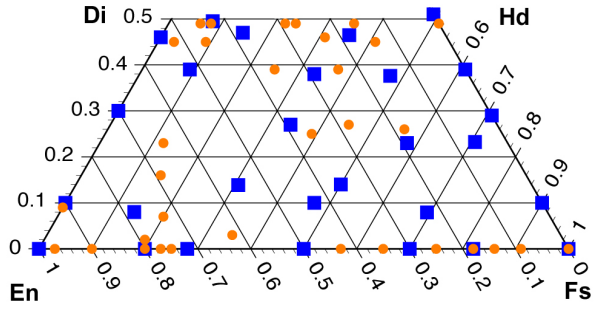

Figure 2. Synthetic pyroxene samples analyzed in this study. Blue squares represent the samples whose spectra will be presented in [10], and the orange dots represent additional spectral data that will be available in that paper but not presented in the figures.

These samples have been studied previously using visible/near-infrared and Mössbauer spectroscopies [11, 12]. The sample numbers (Table 1) may be related to their position on the pyroxene quadrilateral (Fig. 2) through the sample numbers shown on Fig. 3.

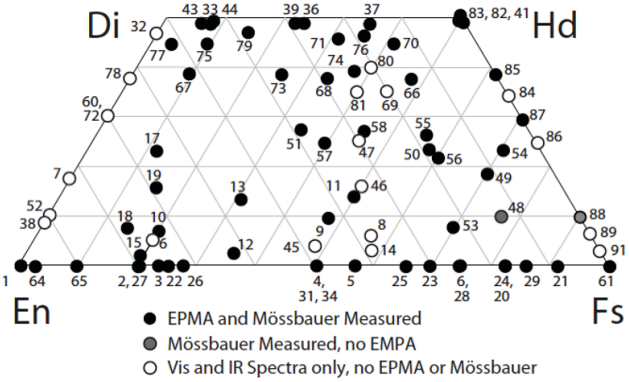

Figure 3. Sample numbers and their compositions (Table 1) shown on pyroxene quadrilateral [from 12].

Spectral Study: The samples were measured at ambient pressure (in a purged environment) in reflectance and emission to understanding the specific and systematic variations of spectral bands related to chemistry and crystal structure as affected by Ca, Mg, and Fe-substitution, and to note the spectral differences between the 2 methods.

The samples were synthesized as fine powders, hence they displayed volume scattering effects [e.g., 13-15]. Reflectivity spectra were obtained on most of these powders. Emissivity spectra were obtained from many of the samples both as powders and after being pelletized to remove the spectral effects of volume scattering within the samples. Table 1 shows which data were obtained for each sample.

NOTE: Although no spectra are shown here, the reflectivity (R) and emissivity (ε) spectra will be shown at LPSC and all of the acquired spectra data (R_{powder}, ε_{powder}, ε_{pellet}) will be available through [10].

Summary: The synthetic pyroxene samples studied represent Ca^{2+}, Mg^{2+}, and Fe^{2+} chemistries over the whole pyroxene quadrilateral. The mid-infrared reflectivity and emissivity spectra acquired thereof show band trends and spectral variations that will be useful for identifying pyroxene compositions in remote sensing data. A manuscript of this comprehensive study is in preparation [10] and will include all of the digital spectra acquired of the pyroxenes (Table 1) for use by other researchers.

Table 1. Synthetic sample compositions measured in reflectance & emission

Sample	Wo	En	Fs	R Powder	ε Powder	ε Pellet
Ca-Mg:						
032*	46	54	0	X	X	X
077	45	52	3	X	--	--
072*	30	70	0	X	--	--
052*	10	90	0	X	--	X
038*	9	91	0	X	--	--
Ca-Fe:						
083	51	0	49	X	--	--
041	49	0	51	X	--	--
085	39	0	61	--	--	X
087	29	0	71	--	--	X
088*	10	0	90	--	--	X
Ca-Mg-Fe:						
037	49	16	35	X	--	--
036	49	27	24	X	--	--
039	49	29	22	X	--	--
033	49	42	8	X	X	X
044	49	43	8	X	--	--
043	49	45	6	X	X	--
079	47	38	15	X	--	--
071	46	23	31	X	--	--
076	46	18	35	X	--	--
070	45	14	41	X	--	--
075	45	46	9	X	--	--
074	39	24	37	X	--	--
073	39	36	25	X	--	--
067	39	52	9	X	--	X
066	38	15	48	X	--	X
068	38	29	33	X	--	X
058	27	28	45	X	--	--
051	27	39	34	X	--	X
055	26	18	56	X	--	--
057	25	36	39	X	--	--
017	23	65	12	X	--	--
050	23	19	58	X	--	--
054	23	6	70	X	--	--
019	16	69	15	X	--	--
011	14	36	50	X	X	--
013	14	56	31	X	--	--
009	10	43	47	X	X	X
053	8	23	70	X	--	--
018	8	78	14	X	X	--
010	7	73	20	X	--	--
Mg-Fe:						
001	0	100	0	X	X	X
064	0	97	3	X	--	--
065	0	90	10	X	--	--
027	0	80	20	X	X	X
002	0	80	20	X	--	X
015	2	79	19	X	X	--
003	0	77	23	X	X	X
022	0	75	25	X	X	X
026	0	72	28	X	X	X
012	3	62	35	X	X	X
004	0	50	50	X	X	--
005	0	43	57	X	--	--
025	0	35	65	X	X	X
023	0	30	70	X	X	X
028	0	25	75	X	X	--
024	0	18	82	X	X	X
020	0	18	82	X	--	--
029	0	14	86	X	--	--
021	0	9	91	X	X	X
061	0	0	100	X	--	--
062	0	0	100	X	--	X
063	0	0	100	X	--	--

* Denotes sample compositions were determined through Scanning Electron Microscope analyses. (All other sample compositions were achieved through electron microprobe measurements.) Colors correspond to Figure 2.

References: [1] Wells P. R. A. (1977) *Cont. Min. Pet., 62,* 129-139. [2] Taylor W. R. (1998) *Neu. Jahr. Min. Abhand. Band, 172,* 381-408. [3] Lindsley D. H. (1983) *Am. Min., 68,* 477-493. [4] Klima R. L. et al. (2008) *Met. Planet. Sci, 43,* 1591-1604. [5] Brucato J. R. et al. (1999) *Astron. Astrophys., 348,* 1012-1019. [6] Hamilton V. E. (2000) *JGR, 105,* 9701-9716. [7] Koike C. et al. (2000) *Astron. Astrophys., 363,* 1115-1122. [8] Chihara H. et al. (2002) *Astron. Astrophys., 391,* 267-273. [9] Ferrari S. et al. (2014) *Am. Min., 99,* 786-792. [10] Lane M. D. et al. (2018) *Met. Planet. Sci.*, in prep. [11] Klima R. L. et al. (2007) *Met. Planet. Sci., 42,* 235-253. [12] Dyar M. D. et al. (2013) *Am. Min., 98,* 1172-1186. [13] Lyon R. J. P. (1964) *NASA Contract Rep., CR-100.* [14] Salisbury J. W. and Wald A. (1992) *Icarus, 96,* 121-128. [15] Lane M. D. (1999) *JGR, 104,* 14099-14108.